J Mater Sci (2011) 46:7883–7894
DOI 10.1007/s10853-011-5776-1

Effect of the SiC particle size on the dry sliding wear behavior of SiC and SiC–Gr-reinforced Al6061 composites

S. Mahdavi · F. Akhlaghi

Received: 12 March 2011 / Accepted: 7 July 2011 / Published online: 20 July 2011

Abstract The effect of size of silicon carbide particles on the dry sliding wear properties of composites with three different sized SiC particles (19, 93, and 146 μm) has been studied. Wear behavior of Al6061/10 vol% SiC and Al6061/10 vol% SiC/5 vol% graphite composites processed by in situ powder metallurgy technique has been investigated using a pin-on-disk wear tester. The debris and wear surfaces of samples were identified using SEM. It was found that the porosity content and hardness of Al/10SiC composites decreased by 5 vol% graphite addition. The increased SiC particle size reduced the porosity, hardness, volume loss, and coefficient of friction of both types of composites. Moreover, the hybrid composites exhibited lower coefficient of friction and wear rates. The wear mechanism changed from mostly adhesive and micro-cutting in the Al/10SiC composite containing fine SiC particles to the prominently abrasive and delamination wear by increasing of SiC particle size. While the main wear mechanism for the unreinforced alloy was adhesive wear, all the hybrid composites were worn mainly by abrasion and delamination mechanisms.

Introduction

Aluminum matrix composites are widely used in engineering applications because of their enhanced mechanical and tribological properties over the unreinforced alloys [1–9]. These composites have gained extensive applications in several sectors such as structural, aerospace, and automotive industries [5–16]. The volume fraction, shape, and size of the reinforcing particles, chemistry of the aluminum alloy as the matrix, and processing route for making these composites influence their final properties which must be optimized for the desired applications [8–10, 17]. Among the hard reinforcing particles, SiC has demonstrated excellent compatibility with aluminum alloys resulting in improved wear resistance of the composites [5, 6, 9–11, 18, 19]. The reinforcing particles support the contact stresses and thereby prevent or reduce the degree of plastic deformation and abrasion [5]. However, these hard particles increase the wear rate of the mating counterface due to their abrasive action, and thus reduce the overall wear resistance of the tribosystem [8, 9, 12, 13, 19]. In order to overcome these problems, a lubricant can be added to the contact surfaces during the sliding process [9, 20]. However, some drawbacks of liquid lubricants include difficulties in accessing some parts of the contact surfaces, leakage of oil from the lubricating system and environmental pollution [9, 14, 20]. Therefore, application of solid lubricant materials such as graphite, molybdenum disulfide, or boron nitride may be beneficial, in reducing the frictional forces and improving tribological properties [7, 12, 13, 18–23]. The Al/SiC/Gr hybrid composites benefit from both SiC and graphite for their hardening and self-lubricating properties, respectively [7, 8, 14, 16, 18–20].

The size of reinforcing particles is an important factor in determining the tribological behavior of such composites. In fact, both the degree of the reinforcing particles fracture and the ease of their detachment from the matrix determine the wear resistance of composites and are influenced by the particle size [5, 17, 20]. However, a systematic study on the

S. Mahdavi (✉) · F. Akhlaghi
School of Metallurgy and Materials Engineering, College of Engineering, University of Tehran, P.O. Box 11155-4563, Tehran, Iran
e-mail: mahdavis@ut.ac.ir

F. Akhlaghi
e-mail: fakhlagh@ut.ac.ir

effect of the size of SiC particles on the tribological properties of Al/SiC and Al/SiC/Gr composites seems to be lacking.

In this study, a new processing technique, namely in situ powder metallurgy (IPM) was used for consolidating Al6061/SiC and Al6061/SiC/Gr composites containing different sized SiC particles. The IPM method is a combination of the stir casting and powder metallurgy (P/M) synthesizing processes in an integrated net shape forming process [16, 21, 22]. It is well known that the production method has a strong influence on the mechanical and tribological properties of such composites via its effects on the matrix grain size, porosity, the distribution of reinforcing particles, and the reinforcement–matrix interfacial properties [10, 16, 20, 21]. The aim of this study is to investigate the effect of SiC particle size on the tribological behavior of Al/SiC and Al/SiC/Gr composites under dry sliding conditions.

Experimental procedure

Specimen preparation

Al6061 alloy with the chemical composition as shown in Table 1 was used as the matrix material. The IPM method was used for preparation of different batches of Al/SiC or Al/SiC/Gr powder mixtures. For this purpose, the appropriate weights of Al ingot along with SiC and/or graphite particles were charged in a clay-bonded graphite crucible. The amount of Al, SiC, and graphite was calculated based on their density values (2.7, 3.2, and 2.2 g/cm^3, respectively) to obtain the required volume fractions of each material in different powder mixtures. The produced powder batches consisted of 10 vol% of SiC particles having three different average sizes of 19, 93, and 146 μm (denoted as: fine, medium sized, and coarse, respectively) and 0 or 5 vol% of flake graphite particles with the average size of 75 μm. Figure 1 shows the typical SEM micrographs of the used SiC and graphite powder particles. The crucible was heated in a resistance furnace and after melting the aluminum at a constant temperature of 710 °C, the mixture was stirred at 1400 rpm for 8 min using a spiral shaped graphite stirrer. During stirring the mixture, the molten aluminum alloy was disintegrated into droplets by the shear forces induced by the impeller at the presence of non-wettable SiC and graphite particles. The mixture was evacuated from the crucible onto a steel flat plate and the alloy was allowed to solidify at ambient temperature and atmosphere. This procedure was performed using different sized SiC particles to produce Al/SiC/Gr and Al/SiC powder mixtures. More details about the IPM process are given elsewhere [16]. The powder particles of 6061 Al alloy were produced by "solid-assisted melt disintegration" (SAMD) technique. The SAMD technique is basically similar to IPM method, but instead of graphite and/or SiC, coarse alumina particles (>710 μm) are used for melt disintegration [24, 25]. The alumina particles were sieved out from aluminum alloy–alumina powder mixtures, and the resultant aluminum alloy powder particles were used for making compacts of the base alloy for the purpose of comparison.

Table 1 Chemical composition (wt%) of 6061 aluminum alloy

Mg	Si	Fe	Cu	Cr	Al
1.12	0.64	0.48	0.33	0.04	Balance

Powder mixtures were cold pressed at a constant pressure of 750 MPa in a steel die on a single acting hydraulic press into cylindrical compacts. The dimensions of the compacts were 25 mm in diameter and 10 mm in height. Green compacts were sintered at 620–630 °C for 60 min in a tubular furnace and under nitrogen atmosphere to provide protection against oxidation of the aluminum matrix. Then, all the samples were solution treated at 550 °C for 2 h before cold water quenching and artificially aged at 170 °C for 7 h.

Density and hardness measurements

The densities of the base alloy compact and different composites were determined using Archimedes' principle. The theoretical densities were calculated using the rule of mixture according to the volume fractions of Al, SiC, and graphite. The porosities of the different composites were evaluated from the difference between theoretical and the measured density of each sample. Hardness measurements were carried out on a Brinell hardness testing machine, using a load of 300 N, and the mean values of at least five measurements conducted on different areas of each sample was considered.

Microscopy

The morphology of the powder mixtures, polished surfaces of composites as well as the wear surfaces and debris were examined by using a Camscan MV2300 scanning electron microscope equipped with energy dispersive X-ray spectroscopy (EDS).

Wear testing

Dry sliding pin-on-disk wear tests were carried out on the composites and unreinforced samples in a laboratory atmosphere at 30–40% relative humidity and the

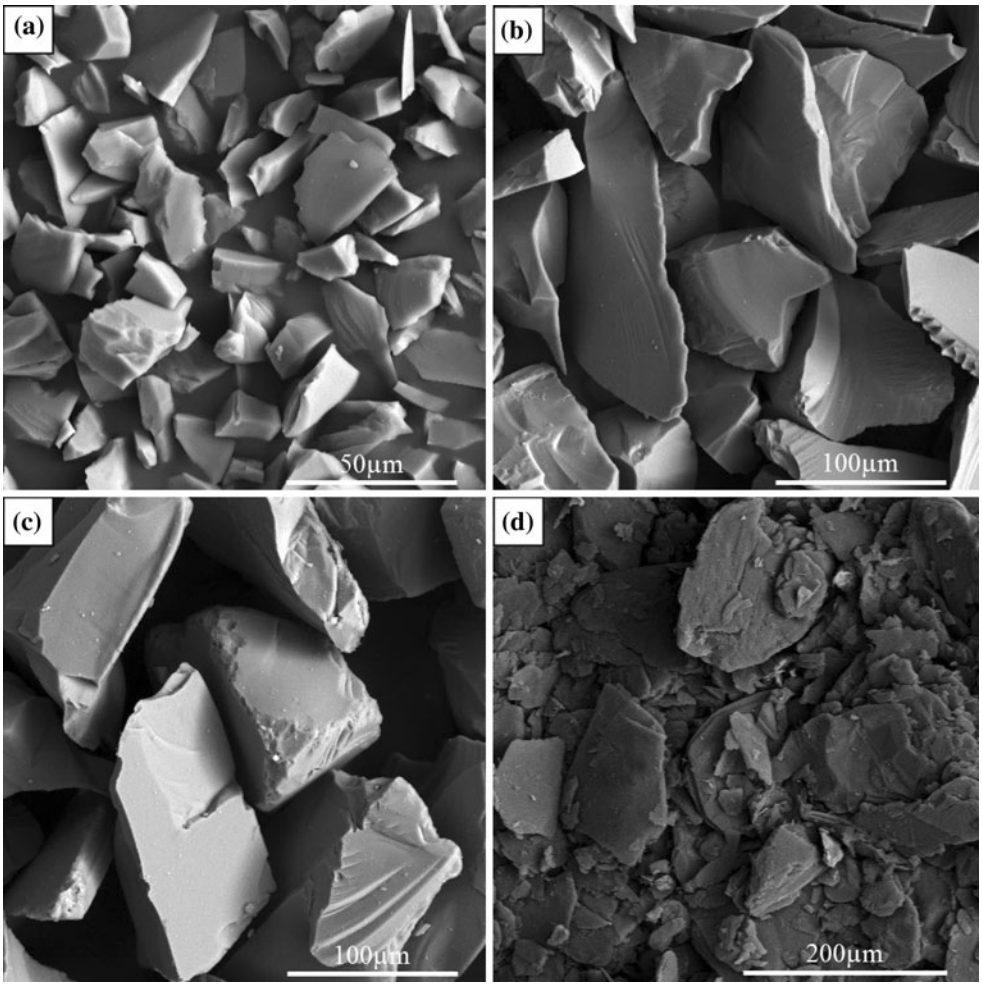

Fig. 1 Typical SEM micrographs of the used powder particles: **a** fine SiC (19 μm), **b** medium sized SiC (93 μm), **c** coarse SiC (146 μm), and **d** graphite

temperature around 25 °C. The rotating test material in the form of disks of diameter 25 mm and height 10 mm were slid against a steel pin (1.5Cr, 1C, 0.35Mn, and 0.25Si) with the hardness of 64HRC having the diameter of 5 mm and height of 20 mm. The surfaces of samples were grounded with SiC paper and cleaned with acetone in an ultrasonic bath before each test. Wear tests were undertaken under the normal load of 20 N (resulting in a normal pressure of 1 MPa), the sliding velocity of 0.5 ms^{-1} and different sliding distances of 250, 500, 750, and 1000 m. The wear tests were carried out using a wear track diameter of 16 mm. The schematic diagram of pin-on-disk testing apparatus is shown in Fig. 2. The weight loss was measured with an accuracy of 0.1 mg, and then converted to volumetric wear loss using the measured density of each material and the total sliding distance. Friction coefficient measurements were made using a transducer to measure the deflection of the pin holder caused by the disk rotation.

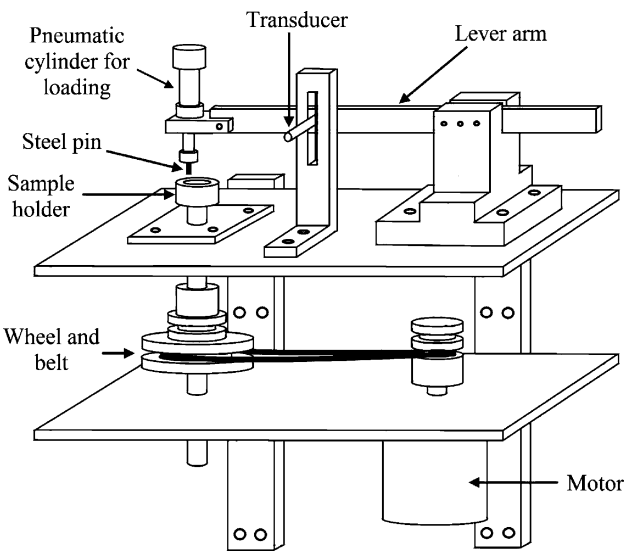

Fig. 2 Schematic view of the pin-on-disk test apparatus

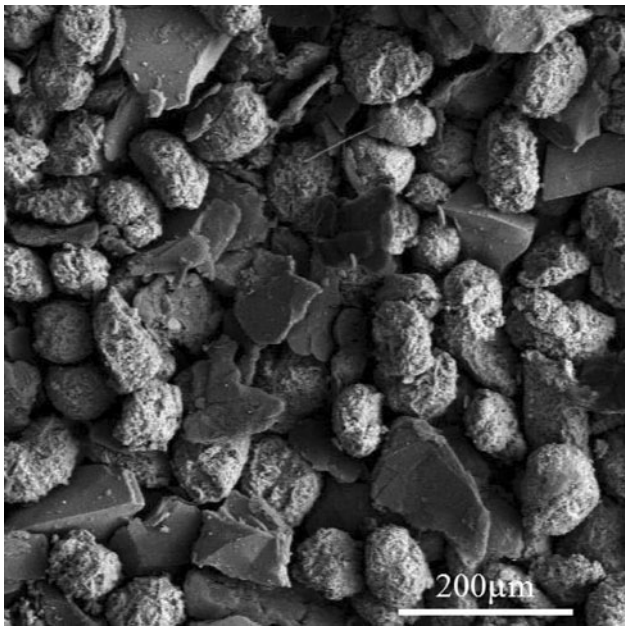

Fig. 3 Typical SEM micrograph of the as-produced powder mixture containing 10 vol% of coarse SiC particles and 5 vol% graphite

Table 2 The median size of the produced aluminum powders in different powder mixtures containing 10 vol% SiC particles

SiC size (μm)	Graphite content (vol%)	D50 (μm)
19	0	319
93	0	347
146	0	364
19	5	305
93	5	318
146	5	336

The system was calibrated by applying known tangential loads and noting pin deflection.

Results and discussion

Powder characteristics

A typical SEM micrograph of the as-produced powder mixture containing aluminum, graphite, and coarse SiC particles is shown in Fig. 3. It is seen that SiC and graphite particles are distributed uniformly within the aluminum powder particles and there is no aggregates of SiC and graphite particles in the mixture. The median size of the produced aluminum particles in different powder mixtures are presented in Table 2. It is clear that smaller aluminum particles are produced by using finer SiC and 5 vol% of graphite particles. This can be attributed to the increased efficiency of melt disintegration by increased surface area of the atomizing medium (fine SiC + Gr particles).

Microstructure of composites

Figure 4a, b shows the typical SEM micrographs of the polished surfaces of composites prepared by using Al/10SiC and Al/10SiC/5Gr powder mixtures containing medium sized SiC particles. This figure shows that reinforcing particles have been distributed uniformly within the matrix alloy, which is an advantage of the IPM method [16, 21, 22]. This uniform distribution improves the mechanical and tribological properties of composites. The dark regions in Fig. 4b represent the graphite particles or voids which were left behind by evacuation of reinforcements from the surface during the polishing process.

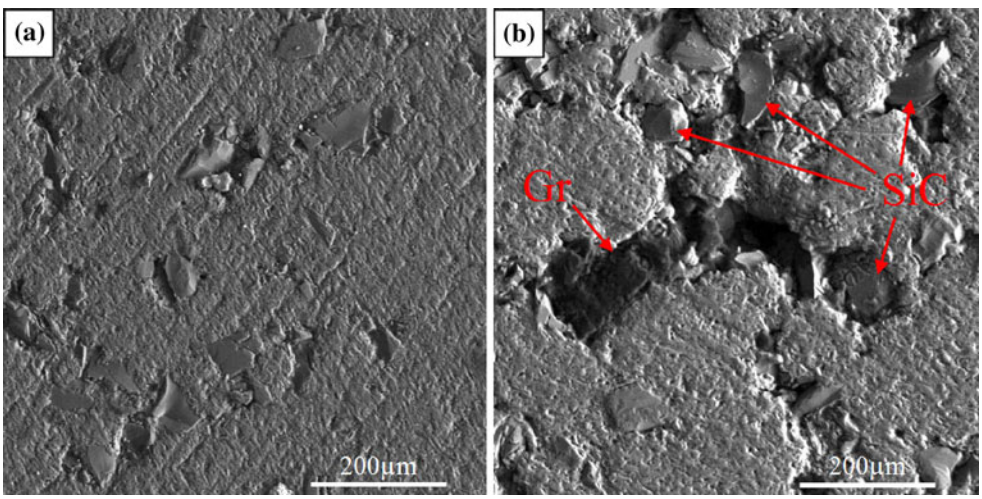

Fig. 4 Typical SEM micrographs of the polished surfaces of **a** Al/SiC and **b** Al/SiC/Gr composites containing 10 vol% medium sized SiC particles

Table 3 The porosity content and hardness values for different samples

SiC content (vol%)	SiC size (μm)	Graphite content (vol%)	Porosity (%)	Brinell hardness (BHN)
10	19	0	3.57	81
10	93	0	2.70	76
10	146	0	1.91	74
10	19	5	2.94	78
10	93	5	2.03	73
10	146	5	1.54	71
Al6061 compact			0.98	63

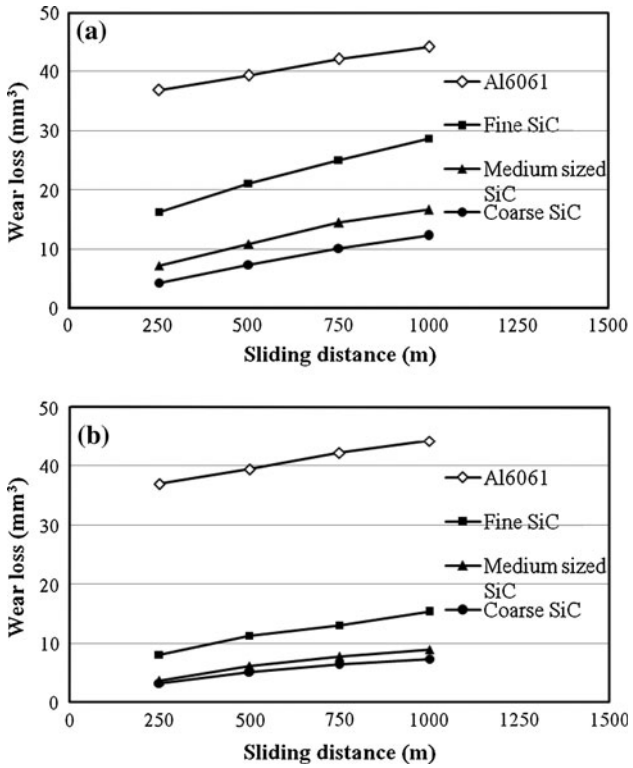

Fig. 5 The variation of wear loss with sliding distance for **a** Al/10SiC and **b** Al/10SiC/5Gr composites

Porosity and hardness of composites

The values of porosity and hardness of unreinforced alloy and composites are presented in Table 3. It is seen that the porosity content and hardness of the unreinforced compact are considerably lower than those of the composites. The hard SiC particles do not flatten by plastic deformation during pressing and therefore preserve the inter-particle voids. Movement and rearrangement of the aluminum powders are also restricted by the reinforcing particles during the compaction process. According to Table 3, for both the Al/SiC and Al/SiC/Gr composites the porosity

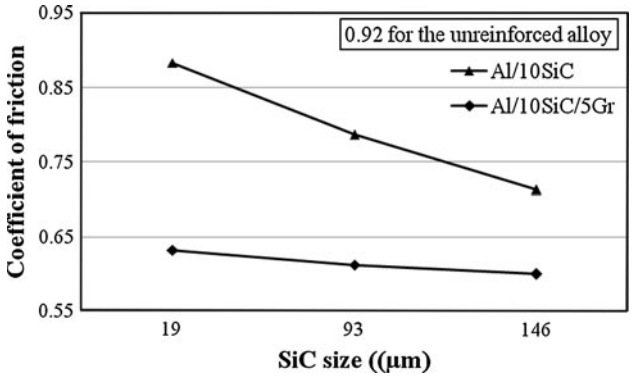

Fig. 6 Variation of the coefficient of friction in different composites with SiC particle size. The data for the base alloy sample is also presented for comparison

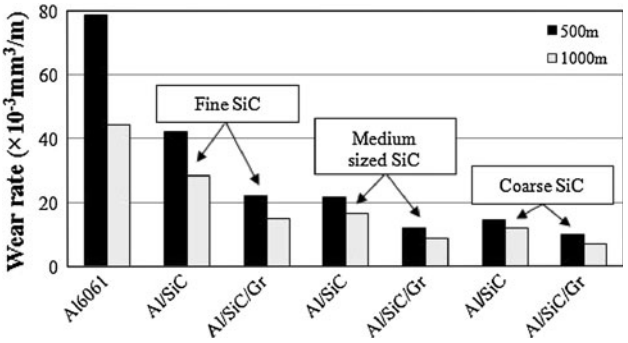

Fig. 7 Variation of the wear rates of Al/SiC and Al/SiC/Gr composites containing different sized SiC particles at the sliding distances of 500 and 1000 m

content and hardness values are decreased by increasing of SiC particle size, which is in agreement with other reports [26, 27]. These results can be attributed to the increased surface area of the finer SiC particles which in turn increases the frictional forces and restricts the movement of particles. Moreover, fine SiC particles are more susceptible to agglomeration which in turn inhibits effective densification. However, graphite as a solid lubricant facilitates movement and rearrangement of the matrix and reinforcing particles, and results in higher densification. Therefore, hybrid composite containing 5 vol% of graphite particles exhibited higher densities as compared with their Al/SiC counterparts.

The higher hardness values obtained for composites as compared with the base alloy compact is due to the presence of hard SiC particles [5, 15, 28]. For both the Al/SiC and Al/SiC/Gr composites, the increased size of SiC particles resulted in decreased hardness values. Again the increased surface area of the finer particles results in increased dislocation density at the Al/SiC interface originated from the coefficient of thermal expansion (CTE) mismatch between these two phases [11, 28]. The lower

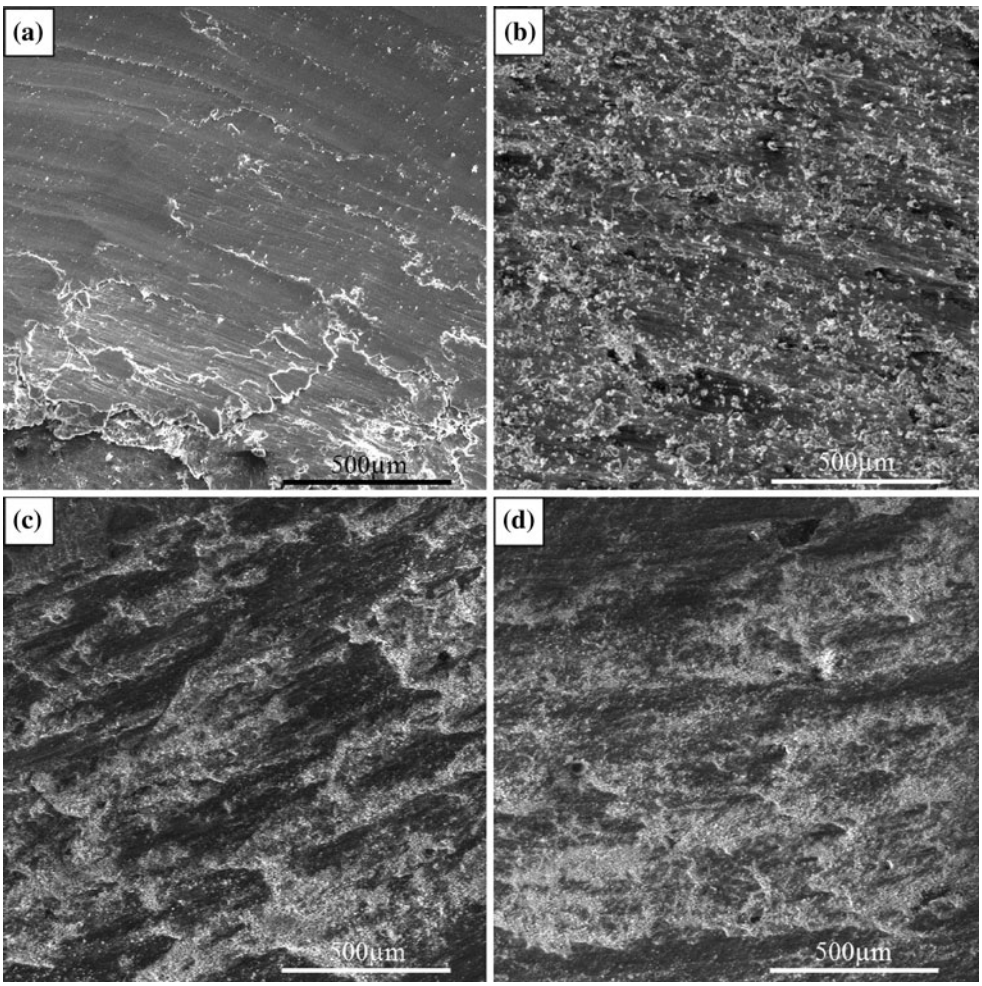

Fig. 8 Typical SEM micrographs of the worn surfaces of **a** unreinforced alloy and **b–d** Al/10SiC composites containing fine, medium sized, and coarse SiC particles, respectively

hardness values for Al/SiC/5Gr hybrid composites as compared with their Al/SiC counterparts are attributed to the soft nature of graphite. It was expected that the decreased porosity level in the hybrid composites result in increased hardness values. However, the effect of soft nature of graphite in reducing the hardness has dominated over the effect of the decreased porosity levels. These results are in agreement with previous observations [13, 14].

Tribological properties

The variation of wear loss with sliding distance for Al/10SiC and Al/10SiC/5Gr composites containing different sized SiC particles is shown in Fig. 5. The wear loss of the base alloy sample is also presented for comparison. It is seen that the composites exhibited lower wear loss as compared with the base alloy. In addition, the increased size of SiC particles resulted in lower wear loss for both composite types. Also the slope of the lines in this figure decreased with the increased size of SiC particles. Similar results have been observed by other investigators [2, 6, 8, 10, 11, 17]. The wear loss of the Al/10SiC/5Gr and Al/10SiC composites containing coarse SiC particles are about 6 and 4 times lower than the unreinforced alloy, respectively. Similar results have also been reported by other investigators [1–5, 8, 10, 14–19]. According to the adhesive wear theory stated by Archard [29], the wear resistance should be deteriorated by decreasing material hardness. However, these results indicate that the increased SiC particle size improved wear properties of composites (Figs. 5, 7) despite of the decreased hardness values (Table 3). This discrepancy can be explained by considering this fact that the Archard's theory is limited to idealized sliding conditions based on a mechanism of adhesion at the asperities. In this theory, the processes of crack nucleation and subsequent growth are disregarded. In fact, in this set of experimental results, the higher porosity

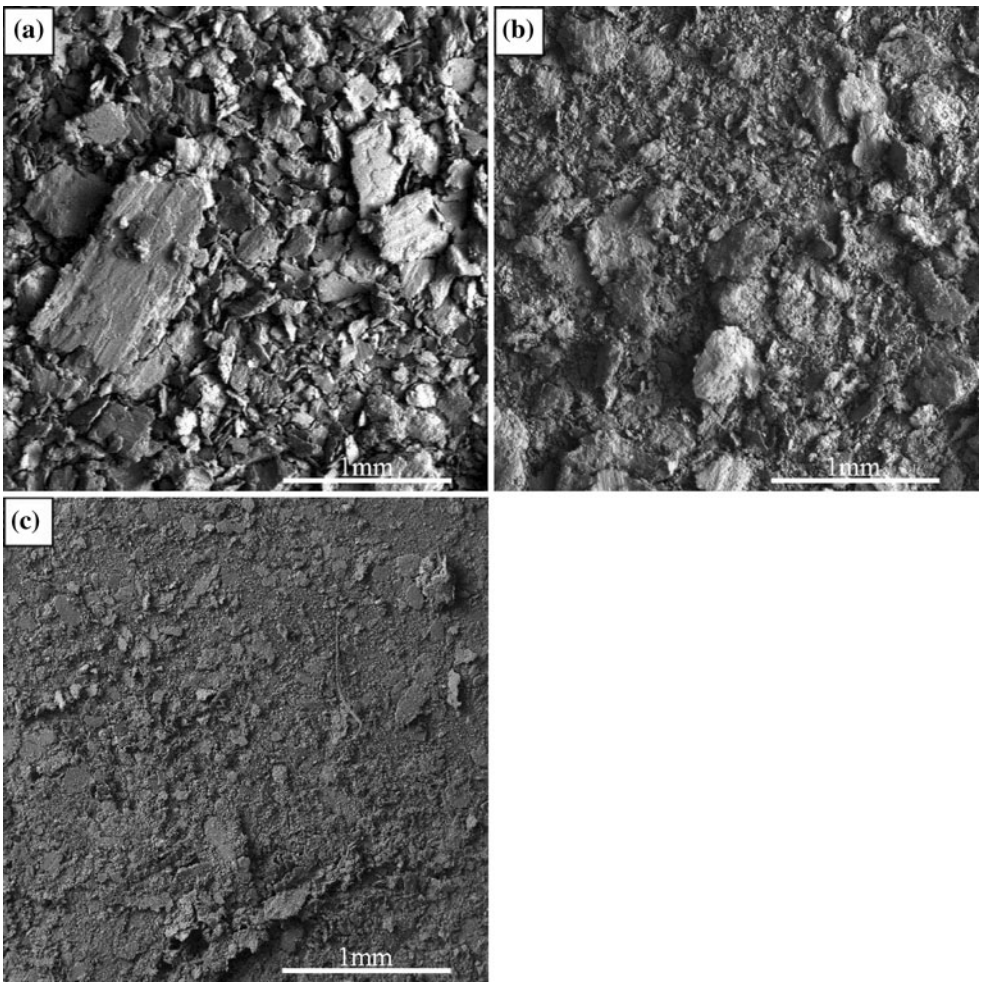

Fig. 9 Typical SEM micrographs of wear debris from **a** base alloy sample, **b** fine SiC contained Al/10SiC composite, and **c** coarse SiC contained Al/10SiC composite

levels of the composites containing finer SiC particles (Table 3), are responsible for deterioration of wear properties [6, 16]. Moreover, the small sized SiC particles on the tribosurface, are not deeply embedded in the matrix alloy and therefore they can be easily pulled out by the steel pin during wear test. However, a relatively high portion of the surface of a coarse SiC particle is embedded in the matrix alloy and it can be remained on the surface during wear test [11]. The increased wear rate with increasing hardness of composites has also been reported by other investigators, and can be attributed to the week interfacial binding between the reinforcement and matrix alloy enhancing the detachment of these particles [2, 3, 9, 17]. Similar mechanism can explain the decreasing of the coefficient of friction by increasing of the SiC particle size, as shown in Fig. 6. The presence of coarse SiC particles on the surface of composites as protrusions protects the matrix from severe contact with the steel pin and reduces their contact area (metal to metal contact), resulting in decreased coefficient of friction [1, 4]. However, the higher porosity of the composites containing finer SiC particles enhances their easy detachment by the steel pin during wear test. Moreover, these fine SiC particles act as the hard third body abrasive and increase the friction coefficient.

Figure 7 indicates that the wear rates of hybrid composites containing different sized SiC particles are lower than those of their Al/SiC counterparts. Similar results have been reported by other researchers [12, 18, 20, 23]. It is also clear from Fig. 6 that friction coefficient of different Al/SiC composites is considerably reduced by 5 vol% graphite addition. The friction force in a tribosystem usually results from the adhesion between counterparts and plowing work [23]. In Al/SiC/Gr hybrid composites, graphite as a solid lubricant material comes onto the surface resulting in the formation of a lubricating film, which prevents metal to metal contact at the sliding surfaces [7, 17, 19, 21] resulting in reduced coefficient of friction as shown in Fig. 6. The reduced slope of the line corresponding to the hybrid

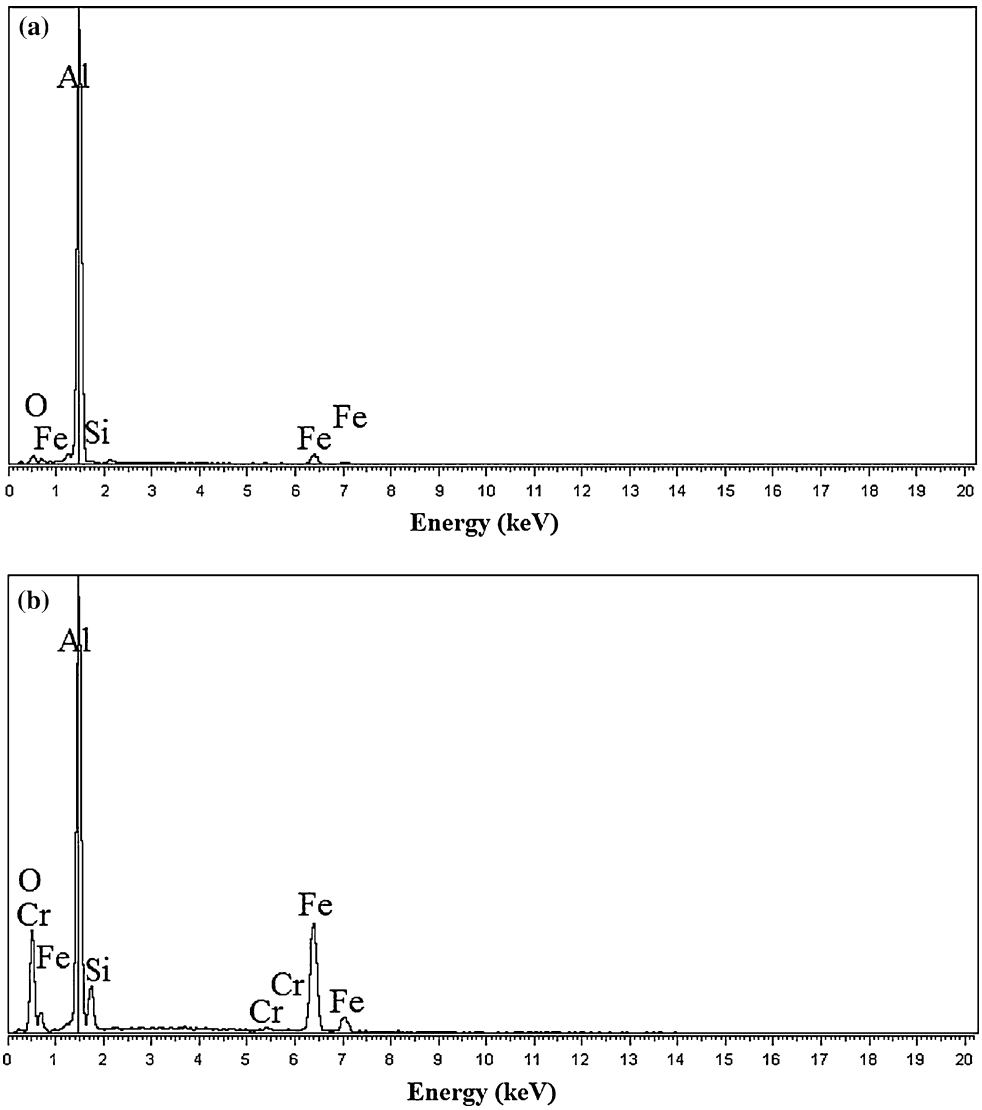

Fig. 10 The EDS spectrums of worn surfaces of Al/10SiC composites containing **a** fine and **b** coarse SiC particles

composites as compared with that of the Al/SiC composites in Fig. 6 can also be attributed to formation of a graphite rich tribolayer which masks SiC particles and reduces their size effect. In addition, this tribolayer reduces the shear stresses transferred to the bulk material and decreases the probability of SiC particles to be pulled out. Therefore, the wear rate or the hybrid composites are lower than their Al/SiC counterparts.

The decreased wear rate with increased sliding distance for the matrix alloy and both composite types as shown in Fig. 7, can be attributed to formation of a more stable smeared layer on the sliding surface which heals the cracks. In case of the matrix alloy, due to a relatively large friction coefficient (0.92 as shown in Fig. 6) and subsequent generation of a large-friction heat, oxidation of the surface and formation of mixed oxide layers is possible. This can be regarded as a reason for the significant decreased wear rate with the increase in sliding distance. However, for the composites, the tribolayer consists of SiC and/or graphite particles (Figs. 8, 11) as well as mixed oxide layers (Fig. 10). Therefore, the more stable wear condition for longer sliding distances resulted in the decreased wear rate. However, this effect is less pronounced for the composites as compared with the unreinforced alloy due to the abrasive action of the detached particles.

Wear mechanisms

A typical SEM micrograph of the worn surface of the base alloy sample is shown in Fig. 8a indicating severe wear by massive plastic deformation. This figure illustrates some wave-like wear patterns created by flow of material demonstrating adhesive wear. The temperature rise on the contact surface during the wear test is an important

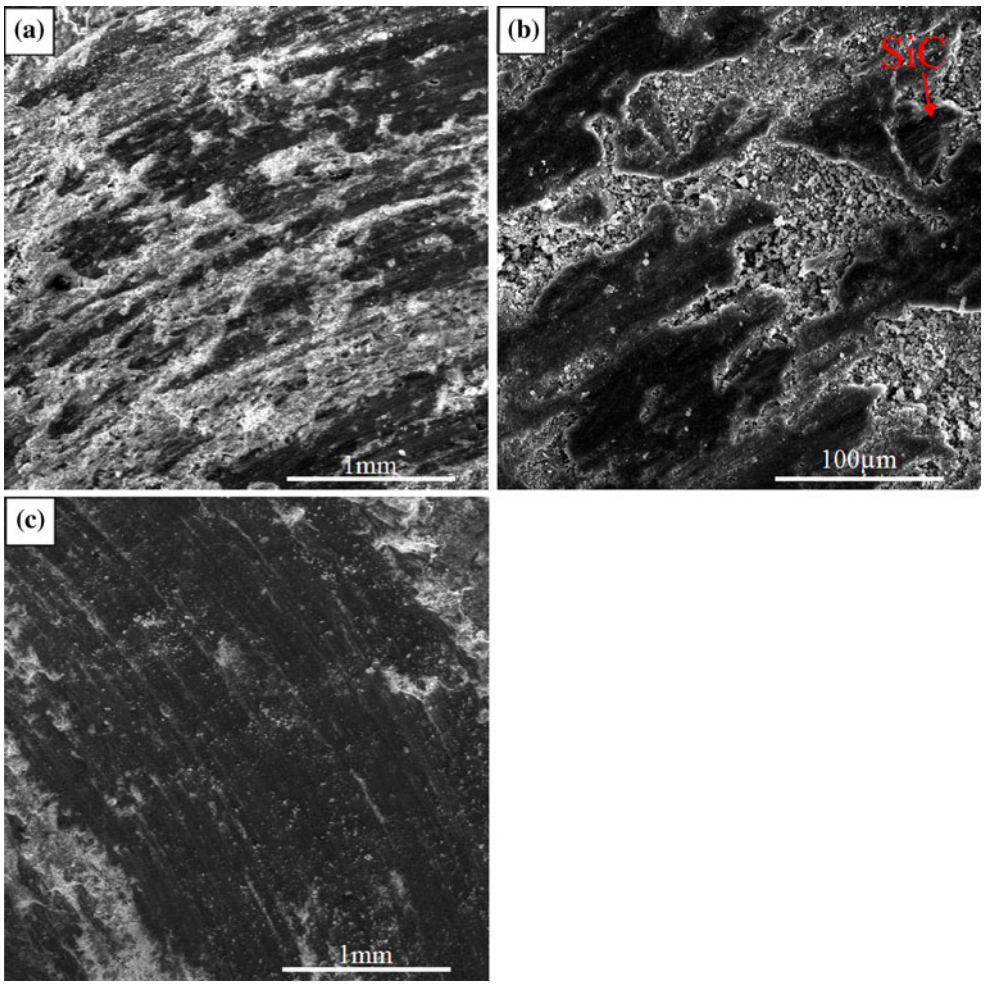

Fig. 11 Typical SEM micrographs of the worn surfaces of Al/10SiC/5Gr hybrid composites containing **a** fine, **b** medium, and **c** coarse sized SiC particles

influential factor in determining the wear mechanism [4, 23, 30]. By increasing this temperature the yield strength of the contacting specimen decreases resulting in softening and creation of adhesive wear, which has also been reported by other authors [1, 3, 8, 14, 23, 30].

The worn surface of fine SiC contained composite, shown in Fig. 8b, indicates massive deformation and granular rough regions. However, protrusion of coarser SiC particles decreases metal to metal contact and causes formation of non-continuous grooves (Fig. 8c, d). The worn surface morphology of the coarse SiC contained composite is more uniform than that of the medium sized one. Incorporation of SiC particles into the aluminum matrix results in increasing of hardness (Table 3) and reduction of real contact area and coefficient of friction (Fig. 6). Therefore, the temperature rise at the surface during wear test is lower for the composites as compared with the unreinforced alloy [4], and as a result, the probability of adhesive wear is weak.

Figure 9 shows the SEM micrographs of the wear debris of the base alloy sample and Al/SiC composites. It is seen that the wear debris of composite samples are smaller than those of the base alloy. As mentioned before, severe adhesion is the predominant wear mechanism of Al6061 alloy sample. The adhesion of the pin together with the shear forces induced to the surface during sliding results in severe plastic deformation at the contact region. Material in the softer asperity deforms in a series of shear bands. When each shear band reaches a certain limit, a crack is initiated, or an existing crack propagates, until a new shear band is formed. When the crack reaches the contact interface, a wear particle is formed and adhesive transfer is completed [7]. This mechanism causes formation of wedge-like shape debris similar to what is seen in Fig. 9a for the base alloy sample. In case of Al/SiC composites, the wear debris morphology is totally changed by increasing SiC particle size from 19 to 146 μm (Fig. 9b, c). Wear debris of fine SiC contained composite consists coarse wedge-like debris

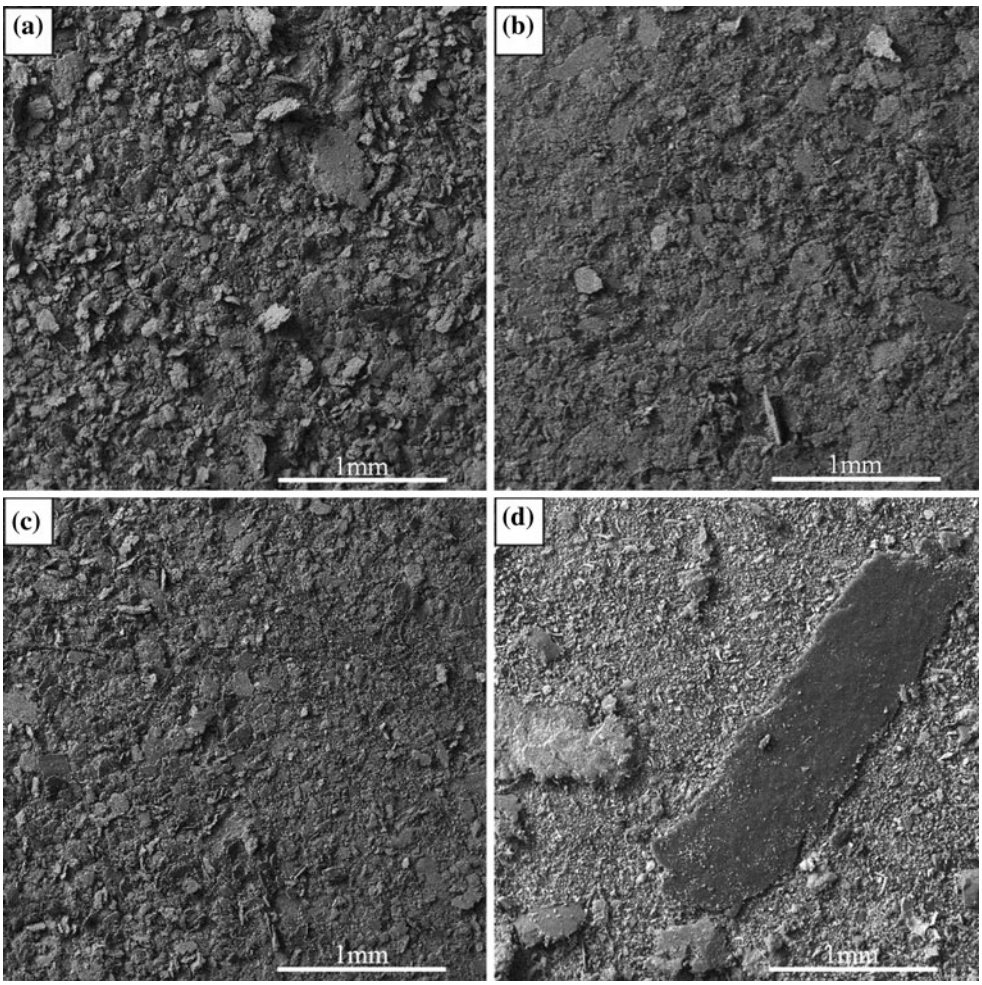

Fig. 12 Typical SEM micrographs of wear debris from Al/10SiC/5Gr hybrid composites containing **a** fine, **b** medium sized, and **c**, **d** coarse SiC particles

together with fine irregular shaped powders. Therefore, the wear mechanism of this composite should be a combination of adhesive and abrasive micro-cutting wear, which has also been reported by other investigators [12]. However, wear debris morphology of coarser SiC contained Al/SiC composites are in the form of small flakes and thin sheets. The micrographs of the worn surfaces and wear debris for the Al/10SiC composites containing coarser SiC particles (Figs. 8c, d, 9c) indicate that abrasive wear and delamination are the major wear mechanisms.

The EDS spectrums of the worn surfaces of Al/10SiC composites (Fig. 10) exhibit higher Fe and O contents for the composite reinforced with coarser SiC particles. These results are consistent with the proposed wear mechanisms for these composites. The partially embedded SiC particles induce milling and abrasion on the steel pin resulting in formation of iron and iron oxide rich fragments transferred on the worn surface of composite. These fragments are also responsible for the decreased coefficient of friction as was observed for coarser SiC contained Al/10SiC composites [2, 18, 30].

The worn surface morphology of hybrid composites is shown in Fig. 11. The presence of continuous grooves indicating that abrasion is the predominant wear mechanism. However, the grooves are larger and deeper on the worn surface of fine SiC contained hybrid composite as compared with the coarser SiC contained ones. These grooves are produced by plowing action of hard asperities on the steel pin and hardened worn debris [30]. Fine SiC particles are more susceptible to be pulled out during the sliding process. These hard particles are trapped between the sample surface and the steel pin, and thus, help to the plowing action. Conversely, coarser SiC particles remain in the matrix for longer times and help the lubricating tribolayer to be retained; similar to what has been shown in Fig. 11b for the medium sized SiC contained hybrid composite.

Figure 12 shows the SEM micrographs of the wear debris of hybrid composites reinforced with different sized SiC particles. It is seen that the wear debris is in the form of thin sheets, indicating that delamination is the main wear mechanism in these composites. However, the debris size

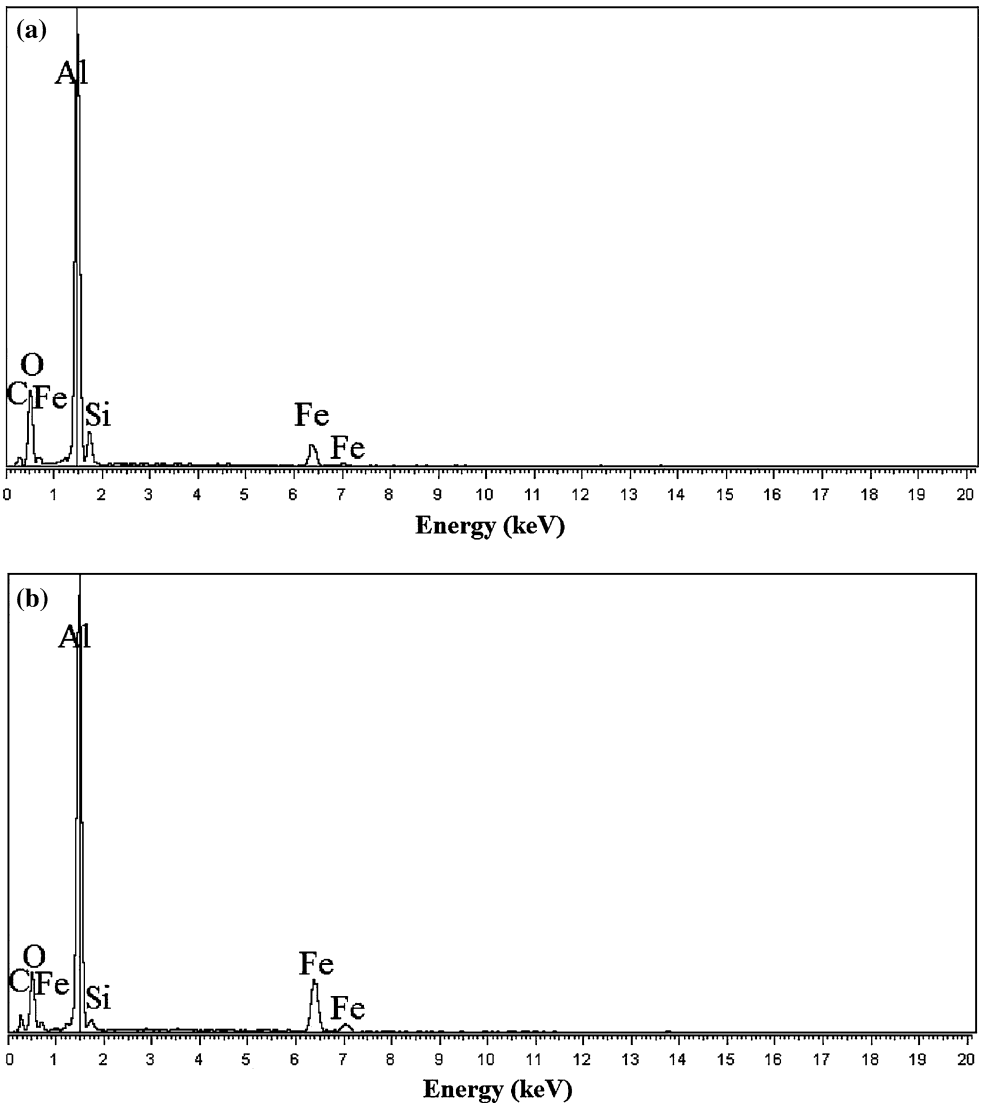

Fig. 13 The EDS spectrums of worn surfaces of Al/10SiC/5Gr hybrid composites containing **a** fine and **b** coarse SiC particles

is decreased by increasing of SiC particle size. Delamination is caused by inhomogeneous plastic deformation at the reinforcement–matrix interfaces, which results in dislocations accumulation, stress concentration, crack formation, and propagation at the interface. These cracks join together and make a flaky wear debris [18, 23]. Therefore, wear debris should be smaller for the fine SiC contained hybrid composite, which has larger number of crack initiation sites as compared with coarser SiC contained composites. However, fine SiC particles are easily pulled out from the matrix and may reduce effective crack initiation sites.

The EDS analysis of the worn surface of Al/10SiC/5Gr hybrid composites reinforced with fine and coarse SiC particles, shown in Fig. 13, exhibit small amounts of Fe and O for both composites. A comparison between Figs. 10 and 13 reveals the decreased Fe and O contents at the worn surfaces of Al/SiC composites by graphite addition attributable to alteration in the wear mechanism. These results imply that the presence of 5 vol% of graphite particles changes the wear mechanism of the fine SiC contained composite from predominant adhesive wear to abrasive. Moreover, the wear mechanisms of the coarser SiC contained composites are similar for the Al/SiC/Gr and Al/SiC composites. It is also clear that the worn surfaces of the hybrid composites are smoother than those of their Al/SiC counterparts (Figs. 8, 11). Moreover, comparing the size of the wear debris in Figs. 9 and 12 reveals that the wear debris resulted from hybrid composites are smaller than those of Al/SiC composites. In the hybrid composites, graphite particles smear out and decrease the coefficient of friction (Fig. 6), resulting in reduction of the wearing surface temperature. Therefore, the shear stresses transferred to the bulk material underneath the tribolayer is reduced [7, 19]. Consequently, the probability of adhesive wear in Al/SiC/Gr hybrid composites is lower than that of the Al/SiC samples. In addition, the SiC particles at the wearing surface of Al/SiC composites are

more susceptible to be fractured and pulled out during the sliding wear. The combination of these mechanisms results in formation of smaller craters and wear debris in the Al/SiC/Gr hybrid composites as compared with Al/SiC ones.

Conclusions

The results can be summarized as follows:

1. The IPM method is a suitable technique for processing of Al6061/10 vol% SiC and Al6061/10 vol% SiC/5 vol% graphite composites containing different sized SiC particles. In these composites the reinforcing particles were distributed uniformly within the matrix alloy.
2. The porosity content, hardness, wear rate, and friction coefficient of Al/10SiC composites decreased by 5 vol% graphite addition. The increased size of SiC particles in the range of 19–146 μm resulted in decreased porosity levels, hardness, wear rate, and friction coefficient of both Al/SiC and Al/SiC/Gr composites.
3. All of the composite samples demonstrated higher porosity content, higher hardness values, lower wear rate, and lower coefficient of friction as compared with the unreinforced alloy. Addition of 10 vol% of coarse SiC together with 5 vol% of graphite particles to the base alloy resulted in reduction in wear rate and friction coefficient by 83 and 35%, respectively.
4. SEM studies of the worn surfaces and wear debris revealed that in the unreinforced alloy the prominent wear mechanism was the adhesive wear. However, in the Al/10SiC composites, by increasing of SiC particle size from 19 to 146 μm the wear mechanism changed from adhesive and micro-cutting to abrasive and delamination. In all the hybrid composites, abrasive wear was the main wear mechanism and was not affected by the SiC particle size.

References

1. Natarajan N, Vijayarangan S, Rajendran I (2006) Wear 261:812
2. Gurcan AB, Baker TN (1995) Wear 188:185
3. Li GR, Zhao YT, Dai QX, Cheng XN, Wang HM, Chen G (2007) J Mater Sci 42:5442. doi:10.1007/s10853-006-0790-4
4. Rao RN, Das S (2010) Mater Des 31:1200
5. Hassan AM, Alrashdan A, Hayajneh MT, Mayyas AT (2009) Tribol Int 42:1230
6. Al-Rubaie KS, Goldenstein H, Biasoli de Mello JD (1999) Wear 225–229:163
7. Basavarajappa S, Chandramohan G, Mukund K, Ashwin M, Prabu M (2006) J Mater Eng Perform 15:668
8. Basavarajappa S, Chandramohan G, Mahadevan A, Thangavelu M, Subramanian R, Gopalakrishnan P (2007) Wear 262:1007
9. Mindivan H, Kayali ES, Cimenoglu H (2008) Wear 265:645
10. Canakci A (2011) J Mater Sci 46:2805. doi:10.1007/s10853-010-5156-2
11. Kumar S, Balasubramanian V (2008) Wear 264:1026
12. Leng J, Jiang L, Wu G, Tian S, Chen G (2009) Rare Met Mater Eng 38:1894
13. Leng J, Jiang L, Zhang Q, Wu G, Sun D, Zhou Q (2008) J Mater Sci 43:6495. doi:10.1007/s10853-008-2974-6
14. Ted Guo ML, Tsao CYA (2000) Compos Sci Technol 60:65
15. Ramesh CS, Safiulla M (2007) Wear 263:629
16. Mahdavi S, Akhlaghi F (2011) J Mater Sci 46:1502. doi:10.1007/s10853-010-4954-x
17. Kiourtsidis GE, Skolianos SM (2002) Wear 253:946
18. Gui M, Kang SB (2001) Metall Mater Trans A 32A:2383
19. Zhan Y, Zhang G (2003) J Mater Sci Lett 22:1087
20. Urena A, Rams J, Campo M, Sanchez M (2009) Wear 266:1128
21. Akhlaghi F, Zare Bidaki A (2009) Wear 266:37
22. Akhlaghi F, Pelaseyyed SA (2004) Mater Sci Eng A 385:258
23. Jun D, Yao-hui L, Si-rong Y, Wen-fang L (2004) Wear 257:930
24. Akhlaghi F, Esfandiari H (2007) Mater Sci Eng A 452–453:70
25. Akhlaghi F, Delshad Khatibi P (2011) Powder Metall 54(2):153
26. Leon CA, Rodriguez-Ortiz G, Aguilar-Reyes EA (2009) Mater Sci Eng A 526:106
27. Hafizpour HR, Simchi A, Parvizi S (2010) Adv Powder Technol 21:273
28. Sivakumar K, Balakrishna-Bhat T, Ramakrishnan P (1998) J Mater Process Technol 73:268
29. Archard JF (1953) J Appl Phys 24:981
30. Mondal AK, Kumar S (2009) Wear 267:458